

HYPERSONIC 3-D FLOW PAST WINGED BODIES

Denny S. CHAUSSEE

NASA Ames Research Center
Moffett Field, CA 94035
USA

ABSTRACT

The 3-D Navier-Stokes equations are used in both a space - and time - marching finite difference code to calculate the hypersonic flow past winged bodies. The bodies are : (1) a blunt ogive-cylinder with a delta wing planform and (2) an elliptical body referred to as the allbody configuration. The grids used for the above configurations were generated with a hyperbolic grid generator. A laminar flow solution for the ogive-cylinder-wing body at a $M = 25$, $\alpha = 3$ deg., and a $q = 1000$ lb/ft**2 is presented. Finally, a $M = 7.4$, $\alpha = 0,10$ deg., laminar flow solution for the allbody configuration is also presented.

INTRODUCTION

There is a great deal of interest in the development of future hypersonic cruise aircraft which would serve the Pacific rim countries by the turn of the century.

In designing these vehicles, the aerodynamic loads and the aerothermodynamics of the configurations need to be known accurately in the hypersonic flight regime. This is important from the stand point of the economics of the design. The more accurately the flowfields are known the lighter the aircraft can be designed which translates into more fuel efficient vehicles.

Computational fluid dynamics (CFD) then becomes an important tool in this design process since an immense amount of flowfield data can be readily computed accurately. Several numerical efforts have been done recently in the area of hypersonic simulations and include for example the works of Edwards (1989), Yamamoto (1988), Corda et al (1988), and Kroll et al (1989). In addition, experimental work is increasing in intensity to provide data for validating and calibrating the CFD tools, i.e. Nomura et al (1988). While the above list of researchers is not comprehensive, it does serve to give an idea of the type of work being concluded throughout the world.

NUMERICAL SCHEME

The time marching algorithm (Rai et al, 1986) which is known as the UWIN code consists of the following physics and numerics. The thin-layer Navier-Stokes equations are solved numerically in a conservation law form to allow for proper shock capturing. The kinematic viscosity is determined from Sutherlands law and the algebraic model of Baldwin-Lomax (1978) would be used for turbulent calculations.

The implicit numerical algorithm is either a Roe or Osher upwind formulation with second order spatial and first order temporal accuracy. In addition, there is a secondary Newton iteration at each time step that permits the solution of the fully implicit finite difference equations. To capture strong shock waves, a TVD formulation of Rai (Edwards 1989) has been incorporated into the algorithm. Also, a zonal approach (Rai 1985) is included within the framework of the code. This consists of two zones each of which can be an independent grid with communication between the two zones occurring across the grid interface. The standard boundary conditions are used. These consist of no slip and a specified wall temperature at the surface. At the outer boundary, the freestream conditions are specified and held fixed during the time iteration process. At the inflow boundary, a specified plane of data is held fixed. In this work, the plane of data was created by a space marching PNS code of Chaussee (1988). At outflow, a zeroth order extrapolation of the conservative variables is used.

GRID GENERATION

The 2-D hyperbolic grid generator is of a type developed by Steger and Chaussee (1980). The technique marches the points away from the body for a specified number of steps. There is some control over the outer boundary location through the specification of control volumes. Internal iterations are used to keep grid lines from crossing as the grids are marched away from the body. This is necessary if there are concave corners in the geometry. In the final

step, the radial lines are accepted and a redistribution of points is done based on a specified stretching function.

RESULTS

Blunt-Ogive-Cylinder-Wing

The first case is the hypersonic flow past an ogive-wing-cylinder. The flow conditions are $M = 25$, $\alpha = 3$ deg. and the dynamic pressure $q = 1000 \text{ lb/ft}^2$. The wall is considered to be cool and a wall temperature is specified accordingly. In this case, the total number of grid points used in the calculation on the wing-body are $80 \times 182 \times 50$. The forebody (the ogive-cylinder nose) solution was obtained using a $19 \times 37 \times 54$ grid. In the description of the grids the first parameter is the axial location, the second is the meridional direction, and the third is the radial direction. A time dependent blunt body code was used to obtain the starting solution at the nose tip of the vehicle. In Fig. 1, the forebody solution is presented for both the crossflow plane and the lee plane of symmetry. The bow

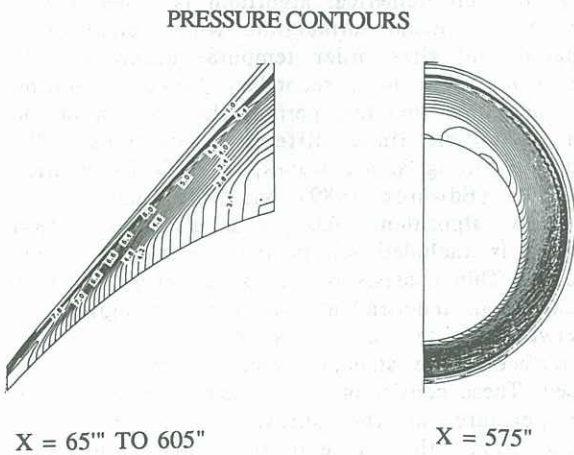


Figure 1. Pressure contours on the forebody

shock wave is captured and is located by the coalescence of the pressure contours. In Fig. 2, the velocity vectors are presented. A very small reverse crossflow component is visible at an $X = 600$ ". The velocity vectors on the leeside show the effect of the viscous phenomena due to the angle of attack of this case.

The wing-body part of the solution is presented next. Figure 3 presents representative cross-sections showing the versatility of the 2-D hyperbolic grid generator. The grid generated is nearly orthogonal. Since the Navier-Stokes equations are cast in a thin-layer form, the optimal grid is of the wrap around type with sufficient clustering at the surface even near concave and convex corners as shown in the figure.

VELOCITY VECTORS

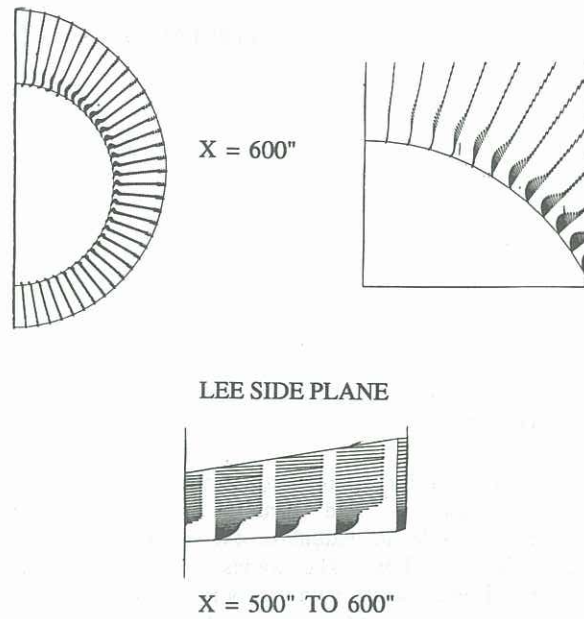


Figure 2. Velocity vectors on the forebody

GRIDS

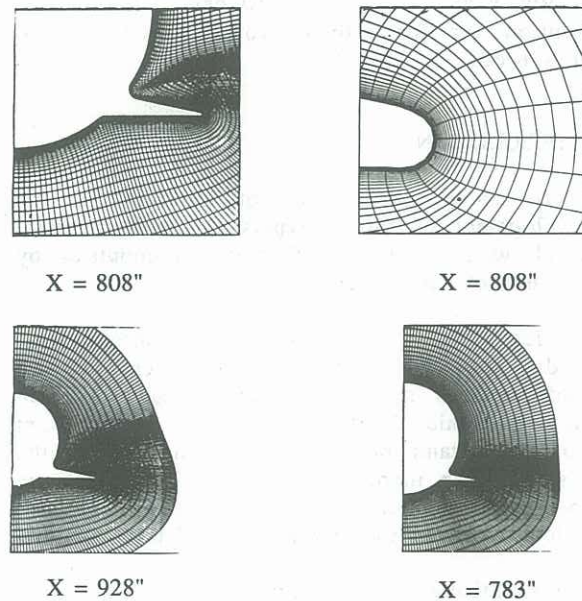


Figure 3. Axial grids at various cross sections.

Pressure contours at various cross sections are presented for the wing-body in Fig. 4. Some of the main features of the flowfield are the strength of the wing shock and the location of the bow shock. Both of the sharp discontinuities are captured by the TVD algorithm of the UWIN code. During the space evolution of the cross sections, the formation of the wing shock and its penetration of the bow shock at an $X = 973$ " are observed in the figure. This demonstrates the shock-shock interaction capturing capability of the code.

PRESSURE CONTOURS

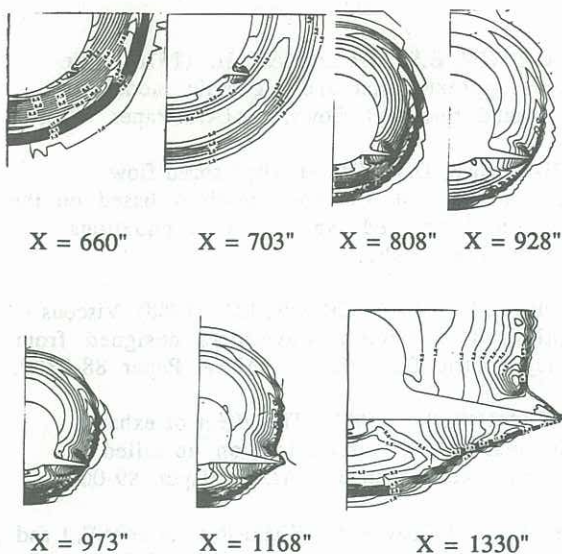


Figure 4. Pressure contours at various cross sections for the winged body.

Figures 5 and 6 present crossflow velocity vectors at different axial stations. In Fig. 5, at an $X = 958$ ", a vortical structure on the leeside is apparent. On the windside, due to the pressure gradient, the flow is migrating towards the windward plane of symmetry. The crossflow velocity vectors at $X = 1330$ " are presented in Fig. 6. The location of the bow and wing shocks are observed by the change in direction of the velocity components. In addition, a crossflow circulation is noted on the leeside and with flow

VELOCITY VECTORS

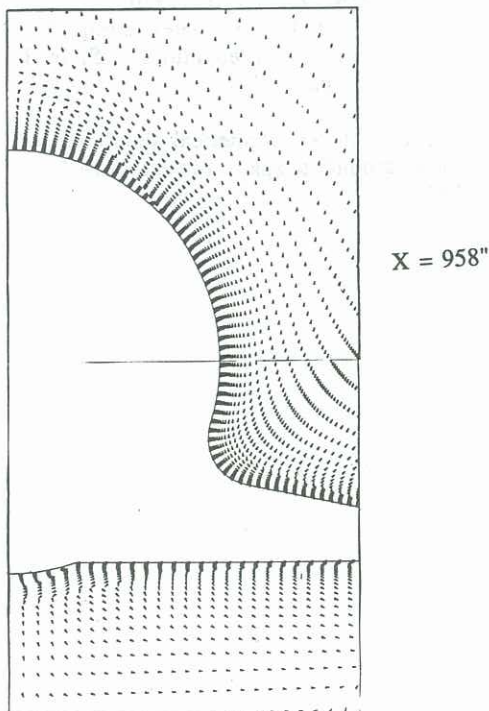


Figure 5. Crossflow velocity vectors.

VELOCITY VECTORS

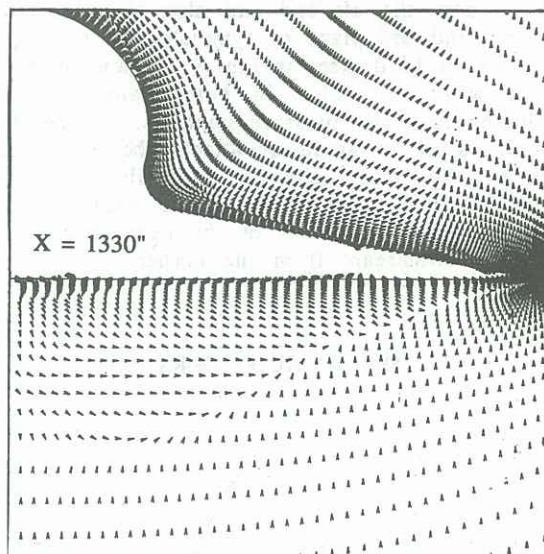


Figure 6. Crossflow velocity vectors.

towards the windward pitch plane also occurring at this cross section.

Allbody Configuration

The last case consists of the hypersonic flow past an allbody configuration. The body consists of an elliptical cone in the forebody and a series of elliptical cross sections in the afterbody region. The axial break occurs at 2/3rds the length of the vehicle. The flow conditions are $M = 7.4$, $\alpha = 0$ and 10 deg. and a specified wall temperature of 560 deg. R. The grid density is $17 \times 92 \times 44$ (same nomenclature as in the previous case).

In Fig. 7, the contours of pressure are presented at a cross section near the aft end of the allbody configuration. The angle of attack is 0 degrees. The bow shock is captured and is located at the coalescence of the pressure contours. A pressure expansion emanating from the slope change at the 2/3rds point is also visible between the body and bow shock wave.

PRESSURE CONTOURS

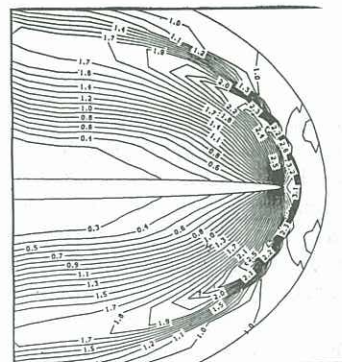


Figure 7. Pressure contours in the cross section

The contours of pressure are presented at a cross section near the aft end and also are presented on the windward plane of symmetry for an angle of attack of 10 degrees in Fig. 8. Again the bow shock wave is visible in both planes as the coalescence of the pressure contours. Since the vehicle is at an angle of attack, the expansion due to the slope change is visible on the windward side only. The profile view of the vehicle shows the extent of the expansion as it extends downstream from the corner.

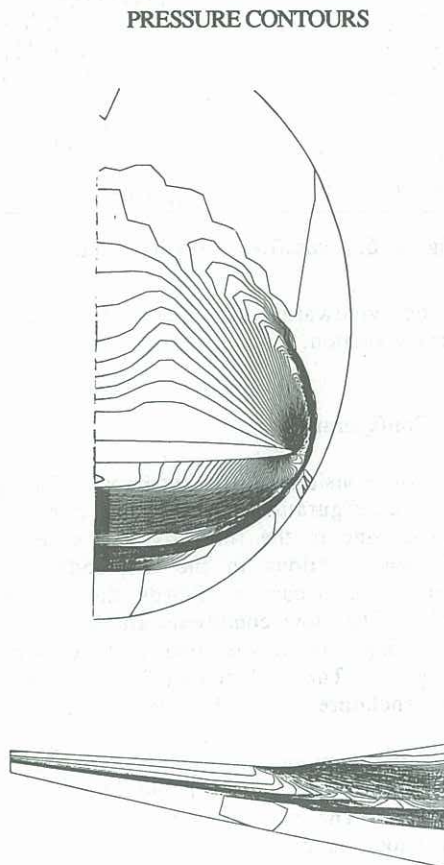


Figure 8. Pressure contours in the cross section

SUMMARY

The 3-D Navier-Stokes equations are used in both a space - and time - marching mode to calculate the hypersonic flow past winged - bodies. It has been shown that the present technique has an excellent shock capturing capability for all speed regimes. In addition, an axial zonal capability is incorporated to make the procedure more versatile. The grid system is created offline using an efficient hyperbolic grid generator which can handle the rapid variations in the body cross sections.

REFERENCES

- BALDWIN, B.S., and LOMAX, H. (1978) Thin-layer approximation and algebraic model for separated turbulent flows. AIAA Paper 78-257.
- CHAUSSEE, D.S. (1988) High-speed flow calculations past 3-D configurations based on the Reynolds averaged Navier-Stokes equations. NASA TM-100082.
- CORDA, S. and ANDERSON, J.D. (1988) Viscous optimized hypersonic waveriders designed from axisymmetric flow fields. AIAA Paper 88-0369.
- EDWARDS, T. (1989) The effect of exhaust plume/afterbody interaction on installed scramjet performance. AIAA Paper 89-0032.
- KROLL, N., ROSSOW, C., SCHERR, S., SCHONE, J. and WICHMANN, G. (1989) Analysis of 3-D aerospace configurations using the Euler equations. AIAA Paper 89-0268.
- NOMURA, S., HOZUMI, K., and KAWAMOTO, I. (1988) Experimental studies on aerodynamic characteristics of SSTO vehicle at subsonic to hypersonic speeds. 16th International Symposium on Space Technology and Science.
- RAI, M.M. (1985) A relaxation approach to patched-grid calculations with the Euler equations. AIAA Paper 85-0295.
- RAI, M.M., and CHAKRAVARTHY, S. (1986) An implicit form for the Osher scheme. AIAA Journal 24 pp. 735-743.
- STEGER, J.L., and CHAUSSEE, D.S. (1980) Generation of body-fitted coordinates using hyperbolic partial differential equations. Siam J. Sci. Stat. Comput., 1, pp. 431-437.
- YAMAMOTO, Y. (1988) Numerical simulation of hypersonic flow around a space plane. AIAA Paper 88-2615.